Gene Discovery Using Mutagen-Induced Polymorphisms and Deep Sequencing: Application to Plant Disease Resistance

Ying Zhu,*,‡,1 Hyung-gon Mang,*,1,2 Qi Sun,†,1 Jun Qian,* Ashley Hipps,*,3 and Jian Hua*,4

*Department of Plant Biology, and †Cornell Computational Biology Service Unit, Cornell University, Ithaca, New York 14853, and ‡State Key Laboratory Breeding Base for Zhejiang Sustainable Pest and Disease Control, Institute of Virology and Biotechnology, Zhejiang Academy of Agricultural Sciences, Hangzhou, 310021, China

ABSTRACT Next-generation sequencing technologies are accelerating gene discovery by combining multiple steps of mapping and cloning used in the traditional map-based approach into one step using DNA sequence polymorphisms existing between two different accessions/strains/backgrounds of the same species. The existing next-generation sequencing method, like the traditional one, requires the use of a segregating population from a cross of a mutant organism in one accession with a wild-type (WT) organism in a different accession. It therefore could potentially be limited by modification of mutant phenotypes in different accessions and/or by the lengthy process required to construct a particular mapping parent in a second accession. Here we present mapping and cloning of an enhancer mutation with next-generation sequencing on bulked segregants in the same accession using sequence polymorphisms induced by a chemical mutagen. This method complements the conventional cloning approach and makes forward genetics more feasible and powerful in molecularly dissecting biological processes in any organisms. The pipeline developed in this study can be used to clone causal genes in background of single mutants or higher order of mutants and in species with or without sequence information on multiple accessions.

ISOLATING causal genes is essential for the understanding of biological processes that mutations in these genes affect. When a mutant phenotype is generated by insertion of a tag (such as a transposon or a T-DNA) in the genome, the causal gene can be identified through isolating sequences flanking the tag. When it is a result of nucleotide sequence change, deletion/insertion, or an epimodification of nucleotide, the causal genes can be identified by their chromosomal locations or maps on the basis of molecular markers linked to these mutations. In the latter case, the mutant organism in an accession/strain/background is crossed to a wild-type (WT) organism in a different accession to generate a population where both the causal mutation and the DNA sequence polymorphisms between the two accessions are segregating. By identifying polymorphisms that are tightly associated with the mutant phenotype, a map position (chromosome location) of the mutation can be defined and candidate mutations can be identified through sequencing the mutation region (Lukowitz *et al.* 2000; Jander *et al.* 2002; Peters *et al.* 2003). This method has been widely used in diverse organisms such as *Drosophila melanogaster* and *Caenorhabditis elegans*. The past two decades have also seen an explosion of use of such map-based cloning in plants to identify important genes in various processes that range from growth and development to biotic and abiotic responses.

Despite being a powerful approach in gene discovery, the classical map-based cloning has several limitations. First, it is dependent on the availability of molecular polymorphisms between genomes of the two accessions. Second, this method is traditionally labor intensive because many mutant plants (often hundreds if not thousands) in a segregating

doi: 10.1534/genetics.112.141986
Manuscript received May 11, 2012; accepted for publication June 8, 2012
Supporting information is available online at http://www.genetics.org/content/suppl/2012/06/19/genetics.112.141986.DC1.
Sequence data from this article can be found in the *Arabidopsis* Genome Initiative or GenBank/EMBL databases under the following accession nos: ABA3 (At1g16540) and SNC1 (At4g16960). Sequencing reads for this study have been deposited to the NCBI Sequence Reads Archive (SRA Submission Accession SRA051235.1).
[1]These authors contributed equally to this work.
[2]Present address: Department of Biology, Texas State University, San Marcos, TX 78666.
[3]Present address: Interdisciplinary Graduate Program, School of Medicine, Vanderbilt University, Nashville, TN 37232.
[4]Corresponding author: 412 Mann Library, Department of Plant Biology, Cornell University, Ithaca, NY 14853. E-mail: jh299@cornell.edu

population need to be genotyped to identify recombinants that refine the mutation position. Third, it requires crossing plants in two different accessions to generate a mapping population. If a mutant phenotype is modified by natural variations between accessions, inferring genotype by phenotype will be complicated. Inconveniently for map-based cloning, natural modification is not uncommon in any species. For example, 5% of the *Saccharomyces cerevisiae* genes that are essential in one accession are not so in another accession, and two to four genes could be required for the phenotypic modification (Dowell *et al.* 2010). In addition, if a new mutant (such as a suppressor or enhancer) is isolated in the background of an existing mutant, the original mutation needs to be introgressed into another accession before a mapping population for the new mutation can be generated. Introgression is a long process as it is done by reisolating the mutant (usually from the F_2 population) from an outcross to a second accession and repeating the process more than five times to obtain a mutant line with the majority of the chromosomes coming from the second accession.

The first two limitations are now overcome by the recent technical advances in next-generation sequencing where vast amounts of sequence information can be acquired in a fast and cost-effective way (Mardis 2008; Shendure and Ji 2008). This technology has revolutionized genomic studies and enabled our understanding of dynamics and functions of cells and population at single-base resolution (Lister *et al.* 2009). Interrogation of whole genome information on various accessions is becoming more affordable and accessible whether a related reference genome is available (Cao *et al.* 2011; Gan *et al.* 2011) or not (Elshire *et al.* 2011). Although it is possible to reveal mutations in a mutant plant by direct whole genome sequencing when a reference wild-type genome is available, it is almost impossible to identify the causal mutation because there are usually numerous base changes irrelevant to the phenotype in a particular mutant. Therefore, combining the traditional mapping with whole genome sequencing in one step becomes a powerful and effective way to clone genes. Instead of sequencing only one mutant plant (as in direct sequencing of a mutant) or analyzing one plant at a time for hundreds of plants (as in traditional map-based cloning), segregants of the same phenotype from the F_2 progenies are pooled for deep sequencing to identify causal mutations in one single step. In *Arabidopsis*, this method has been used for identifying a number of genes. For instance, SHOREmap used 500 mutant F_2 progenies from a cross between a growth defective mutant in the Columbia-0 (Col-0) accession with a wild-type plant in the L*er* accession to identify the causal mutation in one next-generation sequencing run of 20× coverage of the genome (Schneeberger *et al.* 2009). Subsequently, use of pools of much fewer segregants was also successful in identifying genes involved in microRNA precursor processing, cell wall, and growth regulation (Cuperus *et al.* 2010; Austin *et al.* 2011; Uchida *et al.* 2011).

In all these examples of gene cloning with the next-generation sequencing approach, mapping and defining gene location are based on the polymorphisms between two accessions and therefore the third limitation resulting from availability of a proper mapping parent in a different accession still exists. Here, we report the use of pooled segregants from progenies of a backcross to identify causal mutations in a double mutant using next-generation sequencing. A different accession or an introgressed mutant are not needed to create the mapping population because this method relies on polymorphisms generated during mutagenesis. This method therefore has potential for identifying causal mutations in any chemical or physical mutagen-induced mutant even when no traditional mapping parents are available. While we were submitting this article, an independent study identified agronomically important loci in rice with a similar approach (Abe *et al.* 2012), demonstrating the powerful use of this strategy.

Materials and Methods

Plant growth and phenotype analyses

Arabidopsis growth, disease resistance tests, mapping, and protoplast transformation were carried out as previously described (Zhu *et al.* 2010). For EMS (ethyl methanesulfonate) mutagenesis, *Arabidopsis* seeds were treated with 2.5% EMS for 12 hr. Information on markers nga63, ciw12, and M59 are at TAIR (http://www.arabidopsis.org). Primer sequences for the markers JH15 and JHdcaps21 are: JH15-F 5′-CCTGTGTTGGTCATTTGCAC, JH15-R 5′-ACCAATTGCAACAATCATGC, JHdcaps21-F 5′-AACCAAAGTGACTACTAATTCC, and JHdcaps21-R 5′-CGAGAGAAGCTATCCTTCATTGAG. Amount of salicylic acid (SA) and abscisic acid (ABA) were analyzed as previously described (Pan *et al.* 2008).

Next-generation sequencing

F_2 progenies from a cross of *int70 snc1-1* and *snc1-1* were grown and scored at 28°. Equal amount of leaf tissues were collected from each plant and tissues from mutant and non-mutant plants were pooled separately for genomic DNA extraction using the E.Z.N.A. plant DNA Midi kit (OMEGA Bio-tek, Inc, http://www.omegabiotek.com). DNA libraries for Hi-Seq were constructed according to manufacturer instructions (Illumina, http://www.illumina.com). The libraries were run on Illumina Hi-Seq with single reads of 51 bp.

Results

Isolation of temperature-insensitive disease resistance mutants

Plant disease resistance is modulated by temperature and an elevated temperature often renders an otherwise resistant plant susceptible to pathogen invasion (Wang *et al.* 2009). To investigate how temperature affects disease resistance,

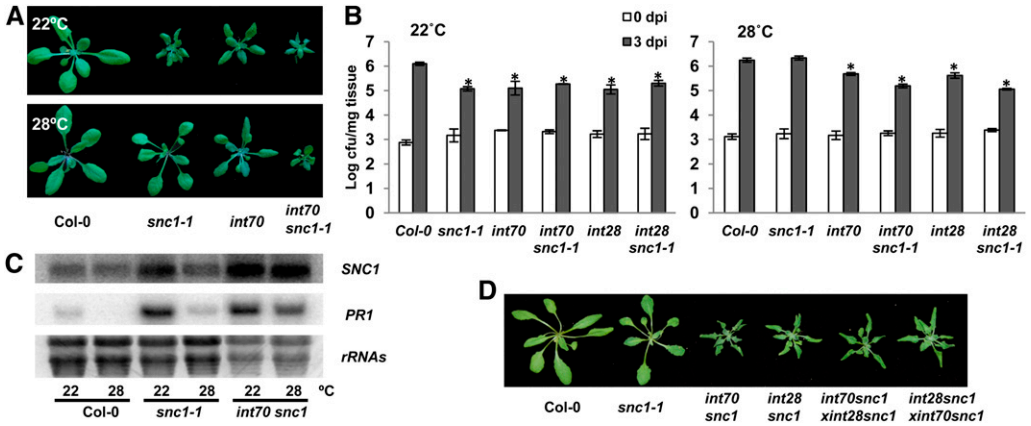

Figure 1 The *int70* and *int28* mutations conferred enhanced disease resistance to *snc1-1* mutants at high temperature. (A) The *int70* mutation confers a dwarf phenotype to *snc1-1* at 28°. Shown are the wild-type Col-0, *int70*, *snc1-1*, and *int70 snc1-1* plants grown at 22° and 28°. (B) The *int70 snc1* and *int28 snc1* double mutants displayed enhanced disease resistance to the virulent pathogen *Pseudomonas syringae pv tomato* (*Pst*) DC3000 at high temperature. Shown are pathogen amounts in Col-0, *snc1-1*, *int70*, *int70 snc1-1*, *int28*, and *int28 snc1-1* grown at 22° (top) and 28° (bottom) at day 0 and day 3 postinnoculation (dpi). Values represent mean ± SD (n = 3). The asterisks indicate a significant difference from the wild-type Col-0 as determined by Student's t-test ($P \leq 0.05$). Similar results were observed in three independent experiments. (C) Expression of *SNC1* and *PR1* was increased in *int70 snc1-1* at 28°. Shown is the RNA blot of total RNAs from the wild-type Col-0, *snc1-1*, and *int70 snc1-1* plants grown at 22° and 28°. *rRNA*'s stained with ethidium bromide were used as a loading control. (D) The *int70* and *int28* mutations are allelic. Shown are the 28° grown plants of the wild-type Col-0, *snc1-1*, *int70 snc1*, *int28 snc1*, a F_1 plant from *int70 snc1* (female) cross to *int28 snc1* (male), and a F_1 plant of a reciprocal cross. The F_1 plants had a similar growth phenotype to those of the two double mutant parents.

we carried out genetic screens for mutants that retain disease resistance at high temperature in otherwise temperature-sensitive disease resistant mutants (Zhu *et al.* 2010). *BON1* (*BONZAI1*) is a negative regulator of a TIR-NB-LRR type of *R* (*Resistance*) gene *SNC1* (*Suppressor of npr1-1*, *constitutive 1*) and the loss of *BON1* function in *bon1-1* leads to activation of plant defense responses (Yang and Hua 2004). The *snc1-1* (or *snc1*) has a missense mutation resulting in an autoactive SNC1, conferring constitutive defense responses (Zhang *et al.* 2003). Both *bon1-1* and *snc1-1* mutants exhibited a dwarf phenotype at 22° but a wild-type growth phenotype at 28° (Yang and Hua 2004) (Figure 1A). These temperature-sensitive autoimmune mutants were mutagenized with EMS and M2 plants were screened at 28° for dwarf phenotypes. Putative *int* (*insensitive to temperature*) mutants were further tested for disease resistance at 28° to identify those with heat-stable disease resistance. Our prior study on the *int102* mutant finds that the TIR-NB-LRR protein SNC1 is the component that confers temperature sensitivity to disease resistance mediated by SNC1 (Zhu *et al.* 2010). Study of another mutant *int173* reveals that mutations in the *ABA2* (*ABA Deficient 2*) gene enhanced disease resistance mediated by *SNC1* and another R gene *RPS4* (*Resistance to Pseudomonas Syringae 4*) at high temperature (Mang *et al.* 2012).

To further investigate the regulation of plant immunity by temperature, we characterized two additional *int* mutants: *int70* and *int28*. Unlike the *snc1-1* plant that is dwarf at 22° but wild type at 28°, the *int70 snc1-1* double mutant showed a dwarf phenotype at both 22° and 28° (Figure 1A) and a similar growth phenotype was found in *int28 snc1-1*. At 22°, both the *int70 snc1-1* and the *int28 snc1-1* double mutants exhibited an enhanced disease resistance to the virulent pathogen *Pseudomonas syringae pv. tomato* (*Pst*) DC3000 similarly to the *snc1-1* single mutant when compared to the wild-type Col-0 (Figure 1B). However, both double mutants exhibited an increased resistance to *Pst* DC3000 at 28° compared to *snc1-1*, which was as susceptible as the wild-type Col-0 at this temperature (Figure 1B). Correlated with the growth and disease resistance phenotype, expression of the defense response marker gene *PR1* as well as the SA-induced *SNC1* gene were upregulated in the *int70 snc1-1* mutant at 28° compared to *snc1-1* (Figure 1C). Because *int70 snc1-1* and *int28 snc1-1* had a similar phenotype and were mapped to a similar region (see below), we tested whether they have lesions in the same gene. The F_1 plants of a cross between these two double mutants exhibited at 28° a dwarf phenotype similar to those of the single mutants, indicating that they are indeed allelic (Figure 1D).

Isolation of the INT70 gene through next-generation sequencing on bulked segregants from a backcross

To identify the molecular bases of enhanced disease resistance by the *int70* mutation at high temperature, we carried out a traditional map-based cloning to identify the causal mutation. The *int70 snc1-1* double mutant in the Col-0 accession was crossed to the wild-type Wassilewskija (Ws) accession. F_2 populations were grown at 28° and the "*int-*" looking plants (segregated at ~1/16) were selected for mapping using SSLP or CAPS markers between Col-0 and Ws (Lukowitz *et al.* 2000; Zhu *et al.* 2010). With bulked segregants of ~50 *int*-looking plants, the *int70* mutation was mapped to a region on chromosome I flanked by markers nga63 and ciw12. Using a total of 498 mutant plants, the mutation was refined to a region between markers JHdcaps21 and JH15, but no further recombinants could be identified for inner markers M59 or JH16 (Figure 2A). A second mapping cross was made with between *int70 snc1-1* and the wild-type L*er* plants, but again no further recombinants could be identified internal to JHdcaps21 and JH15 from hundreds of *int*-looking segregants. Thus,

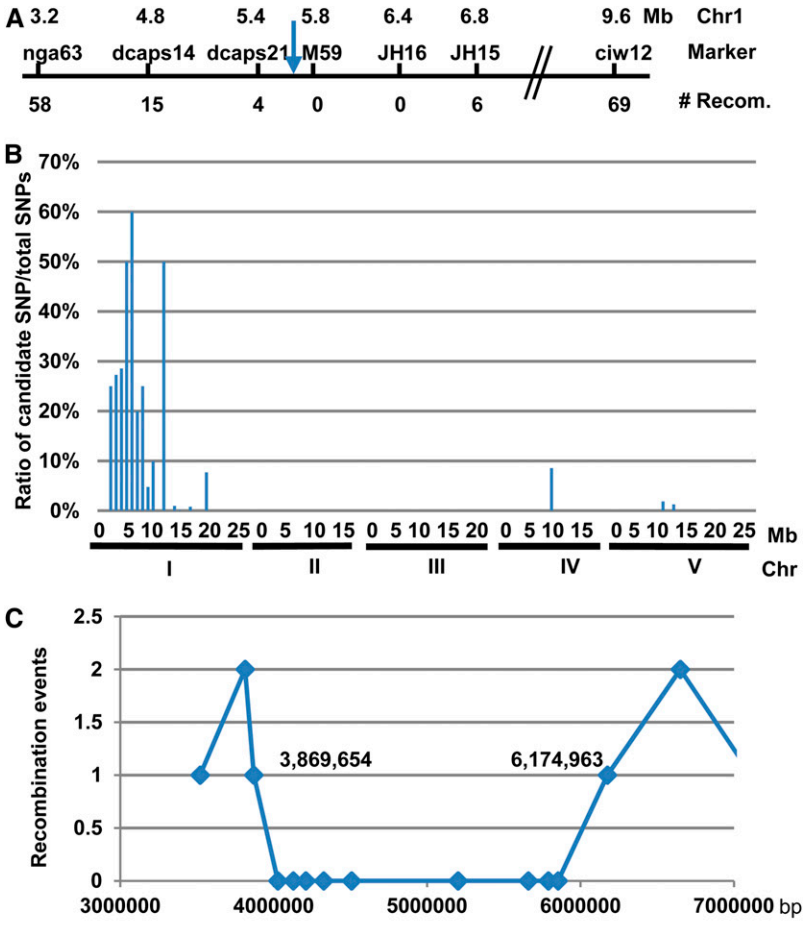

D

SNP	Position (nt)	Ref Allele	Alt Allele	Gene	Type of Alteration	Changes
1	4127172	C	T	AT1G12160	nonsynonymous SNV	T->I
2	4209262	C	T	AT1G12370	upstream	
3	4325416	C	T	AT1G12700	nonsynonymous SNV	R->K
4	4507147	T	A	AT1G13200	downstream	
5	4507150	A	C	AT1G13200	downstream	
6	5659497	T	A	AT1G16540	stop codon	Y->stop
7	5701117	A	C		intergenic	
8	5789700	C	T	AT1G16920	upstream	
9	5853244	C	T	AT1G17120	synonymous SNV	

Figure 2 Mapping and cloning of the *int70* mutation. (A) Traditional mapping of the *int70* mutation. Shown are the molecular markers and their positions on chromosome I around the *int70* region. Close to 500 mutant plants from the progenies of a cross of *int70 snc1-1* (in Col-0) with the wild-type Ws were used to define the position of *int70*. The number of plants with recombination events at these markers is indicated. The arrow indicates the *int70* mutation position. (B) Plot of normalized candidate SNP counts along the five chromosomes. Shown is the ratio (in percentage) of number of candidate SNPs *vs.* total number of the SNPs in a 1-Mb window. Candidate SNPs are defined as having the nonreference allele being >90% in the mutant pool and <50% in the nonmutant pool. (C) Recombination events detected near the peak of candidate SNPs. *X*-axis is the nucleotide position on chromosome I and the *Y*-axis is the number of reference alleles found in the mutant pool. Each positive SNP is represented by a square. (D) Annotation of all nine candidate SNPs in the defined *int70* region. Shown are the base position, sequence of the reference allele, sequence of the nonreference allele, its associated gene, type of alteration, and predicted amino acid change for each SNP.

there appears to be a recombination suppression in the region of 1.4 Mb between JHdcaps21 and JH15.

The recombination suppression might have been due to a number of reasons such as a high level of DNA sequence polymorphisms between accessions or large inversions induced by EMS. We thus decided to try using bulked segregants from F_2 progenies of a backcross in the same accession background combined with next-generation sequencing for mapping and gene identification. The *int70 snc1-1* double mutant in Col-0 was crossed to the original *snc1-1* mutant in Col-0, and the *int70 snc1-1* double mutant segregated at one out of four in the F_2 progenies grown at 28°. Approximately 25 *int*-looking plants and 50 wild-type–looking plants were collected and pooled, respectively. Genomic DNAs were extracted and purified from these mutant and nonmutant pools and libraries constructed from these DNAs were run in a single lane on the Illumina Hi-Seq machine with single-end reads of 51 bp.

We obtained 40,584,342 reads from the mutant pool and 52,614,692 reads from the nonmutant pool, which are on average 11× and 14× coverage of the *Arabidopsis* genome, respectively (Supporting Information, Figure S1A). The sequence reads from the two samples were aligned to the Col-0 reference genome (TAIR v10) by the software BWA (Li and Durbin 2009), a fast program to map short reads on a reference genome. SAMtools-mpileup (Li *et al.* 2009) was used to identify potential SNPs at each position along the five chromosomes. For most of the chromosome regions, 5–10 single nucleotide polymorphisms (SNPs) or small insertions and deletions (INDELs) were identified per

megabase and the medium SNP/INDEL count is eight per megabase, indicating one nucleotide sequence difference every 125 kb between *int70 snc1* and the wild-type Col-0 (Figure S1A). Several chromosome regions exhibited an extremely high number of SNP/INDELs, and they mostly resided in regions with more sequence read coverage (Figure S1B). Very likely these regions contain repetitive sequences, and misalignment of sequence reads could result in false positive SNP/INDELs. The total number of SNP/INDELs is thus estimated to be ~950 on the basis of eight SNP/INDELs per megabase and 119 Mb per genome. Almost all the polymorphisms should have been induced during mutagenesis on *snc1-1* by EMS (12 hr at 2.5%) because most of the background mutations in the starting strain *snc1-1* should have been cleaned by backcrosses. This mutation number is consistent with the earlier TILLING study where ~1000 mutations were found to be induced by EMS per genome (Colbert *et al.* 2001).

We mapped the causal mutation on the basis of the frequency of the nonreference (different from the wild-type Col-0 reference) allele of a SNP/INDEL in the mutant pool and the nonmutant pool. This frequency should be 50% in both pools for most of the SNP/INDELs. However, if the nonreference allele of a SNP/INDLEL is the causal mutation, its frequency should be 100% in the mutant pool and close to 33% in the nonmutant pool. In addition, SNP/INDELs linked to the causal gene should also show a high frequency of nonreference alleles in the mutant pool. After empirically testing frequency setting to maximize detection sensitivity, we defined candidate SNP/INDELs (causal and its linked ones) as having the nonreference allele >90% frequency in the mutant pool and <50% in the nonmutant pool. A PERL script was developed to quantify nonreference allele frequency at each polymorphic site and to filter SNPs on the basis of allele frequency. Count of candidate SNP/INDELs was normalized by count of total number of SNP/INDELs in the same region, and the ratio was plotted along the five chromosomes using a 1-Mb sliding window. This normalization effectively reduced noises from false positive SNPs in the repetitive genomic region. This count ratio plot readily revealed one major peak on chromosome I, indicating the position of the *int70* mutation, which is consistent with the result from the traditional mapping (Figure 2B).

Closer inspection of SNP/INDELs near the peak revealed recombination events that refined the position of *int70* mutation on chromosome I (Figure 2C). A total of nine SNPs in that region were found to have the nonreference allele 100% in the mutant pool and <50% in the nonmutant pool. Flanking these nine SNPs and at positions 3,869,654 bp and 6,174,963 bp, respectively, two SNPs had one reference allele in the mutant pool, indicating recombination events between *int70 snc1-1* and *snc1-1* at these two sites. On the basis of annotation by ANNOVAR (Wang *et al.* 2010), nonreference alleles of five of nine SNPs in the *int70* region were alterations in the intergenic or noncoding regions, three caused nonsynonymous mutations, and one at position 5,659,497 presumably caused a stop codon that made it a good candidate for *int70* mutation (Figure 2, A and D). The reference sequence of this SNP in the wild-type Col-0 is T, and all four reads in the control pool are T, while all nine reads in the mutant pool are A. This mutation resides at nucleotide 33 (translation start being 1) in the first exon of At1g16540, leading to a predicted change of Tyr11 to a stop codon (Figure 3A).

Confirmation of ABA3 as the INT70 gene

This gene At1g16540 was previously identified as *LOS5* or *ABA3* essential for ABA biosynthesis (Xiong *et al.* 2001). It encodes a molybdenum cofactor sulfurase that catalyzes the generation of the sulfurylated form of MoCo, a cofactor required by aldehyde oxidase that functions in the last step of ABA biosynthesis (Bittner *et al.* 2001). If *INT70* is *ABA3*, *int28* should also contain a mutation in the *ABA3* gene. Sequencing the *ABA3* gene in the *int28 snc1* mutant indeed revealed a G nucleotide (at 1415 position of cDNA) in exon 12 substituted by an A nucleotide leading to a missense mutation of arginine 472 to lysine (Figure 3B). This R472K mutation is close to the G469E mutation found in *aba3-1*.

To further verify that mutations in *ABA3* are indeed the causal mutations of *int70* and *int28*, we crossed *aba3-1* with *snc1-1* and isolated the *aba3-1 snc1-1* double mutant. This double mutant had a dwarf phenotype at 28° similar to those of the double mutants *int70 snc1-1* and *int28 snc1-1* (Figure 3B). We thus conclude that *ABA3* is the *INT70/INT28* gene and renamed *int70* as *aba3-21* and *int28* as *aba3-22*.

The *aba3-21* mutant is presumably a null mutant, due to a predicted stop codon in the very beginning of the ABA3 protein. We analyzed the ABA amount in the *aba3-21* single and *aba3-21 snc1-1* mutant and found that the ABA level is ~30% that of the wild-type Col-0 (Figure 3C). The amount of SA is found to be higher in the *aba3-21 snc1-1* double mutant at 28° compared to the wild-type Col-0 or the *snc1-1* single mutant (Figure 3D), which is correlated with an enhanced disease resistance in the *aba3 snc1* mutants at high temperature (Figure 1C). Interestingly, SA amount is higher in *aba3-21* than in Col-0 at both temperatures (Figure 3D), which might account for an enhanced disease resistance to *Pst* DC3000 in the *aba3* single mutants *aba3-21* (*int70*) and *aba3-22* (*int28*) compared to the wild-type Col-0 (Figure 1B).

Nuclear accumulation of SNC1 proteins in aba3-21

High temperature inhibits nuclear accumulation of the SNC1 protein and therefore inhibits defense responses (Zhu *et al.* 2010). Enhanced nuclear accumulation of the SNC1 protein at high temperature was found to confer *int* phenotypes caused by a missense mutation in *SNC1* and an ABA-deficient mutant *aba2* (Zhu *et al.* 2010; Mang *et al.* 2012). We therefore analyzed the subcellular distribution of various forms of SNC1:GFP fusions in the *aba3-21* mutant. Protoplasts were isolated from mesophyll cells of the wild-type Col-0 and the

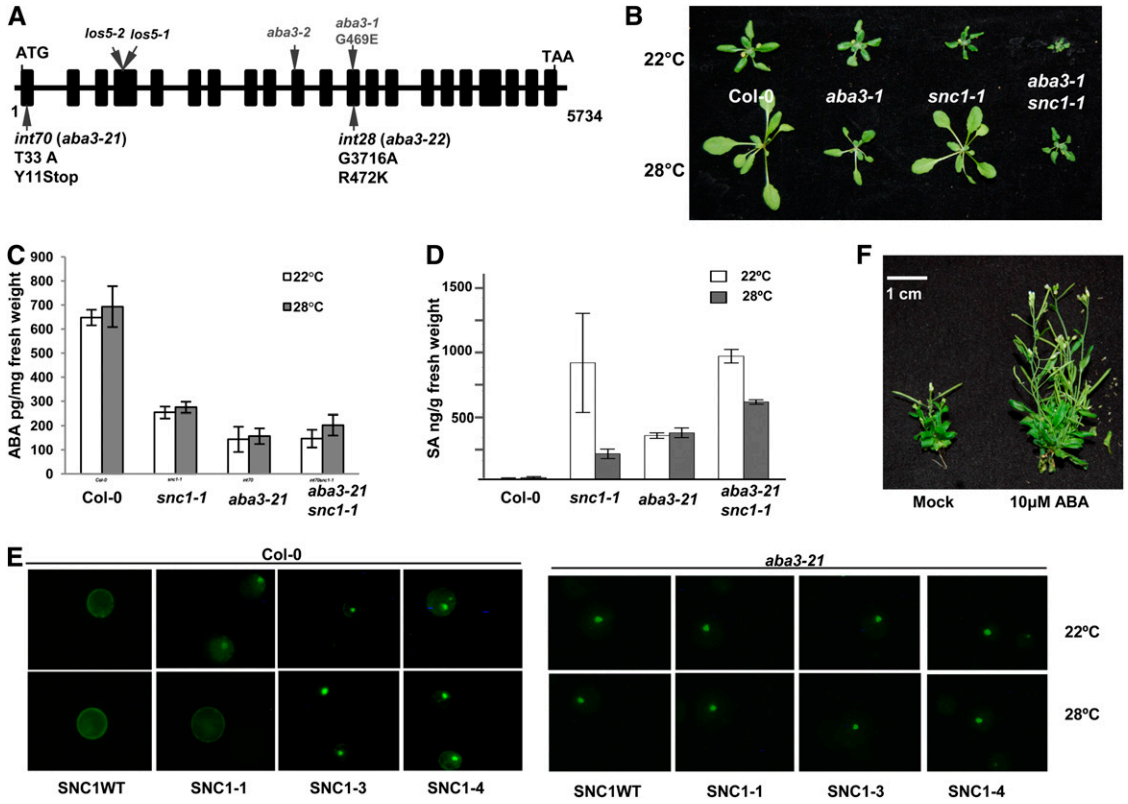

Figure 3 The amount of ABA affects *SNC1*-mediated disease resistance. (A) Mutations in the *ABA3* gene in *int70* and *int28*. Shown is the diagram of the gene structure of ABA3. Boxes represent coding sequences and lines represent introns or 5′ and 3′ untranslated regions of the *ABA3* gene. Nucleotide changes and the predicted amino acid changes in *int70* and *int28* are indicated. Mutation positions of earlier *aba3* alleles (*los5-1*, *los5-2*, *aba3-1*, and *aba3-2*) were also indicated for comparison. (B) Mutation of *aba3-1* confers *int* phenotype to *snc1-1*. Shown are wild-type Col-0, *aba3-1*, *snc1-1*, and *aba3-1snc1-1* plants grown at 22° and 28°. (C) The *int70* mutant is deficient in ABA. Shown are ABA levels in the wild-type Col-0, *snc1-1*, *int70*, and *int70 snc1* plants before bolting grown at 22° and 28°. (D) SA is accumulated to a high level in the *aba3-21 snc1-1* mutant. Shown is the amount of SA in the wild-type Col-0, *snc1-1*, *int70*, and *int70 snc1* plants grown at 22° and 28°. (E) Expression of GFP fusions of various SNC1 forms at 22° and 28° in protoplasts isolated from the wild-type Col-0 and *aba3-21*. Shown are GFP images from representative protoplasts. At 28°, all forms of SNC1:GFP (including SNC1WT, SNC1-1, SNC1-3, and SNC1-4) proteins had a very strong nuclear accumulation in *aba3-21* while only SNC1-3 and SNC1-4 had a strong nuclear accumulation in the wild-type Col-0. (F) ABA spray partially rescued the growth defect of *snc1-1* at 22°. Plant on the right was sprayed with 10 μM ABA twice a day for 3 days at week 4 while plant on the left was sprayed with buffer. Shown are their growth phenotypes at 6 weeks old.

aba3-21 seedlings, and GFP fusions of various SNC1 forms under the control of the strong CaMV 35S promoter were expressed in these protoplasts incubated at 22° and 28°, respectively. The SNC1 forms include the WT, temperature-sensitive autoactive (SNC1-1), and temperature-insensitive autoactive (SNC1-3 and SNC1-4). As reported earlier, SNC1 WT and SNC1-1 had a very strong nuclear accumulation at 22° but not 28°, while SNC1-3 and SNC1-4 had a strong nuclear accumulation at both temperatures (Zhu *et al.* 2010) (Figure 3E). Strikingly, in *aba3-21*, all SNC1 forms had a high nuclear accumulation at both 22° and 28° (Figure 3E), correlating with an enhanced disease resistance in the *aba3* mutants. This further supports the notion that ABA deficiency enhances nuclear accumulation of the R protein SNC1 and consequently confers heat-stable disease resistance.

While ABA deficiency enhances disease resistance mediated by *SNC1*, application of ABA apparently suppressed defense responses induced by the autoactive *snc1-1* mutant gene. When the *snc1-1* plants grown at 22° were sprayed with 10 μM of ABA twice a day for 3 days at 3 weeks old, these plants were much larger 2 weeks later than the *snc1-1* sprayed only with buffer control (Figure 3F). This effect is consistent with the earlier finding that ABA application decreased nuclear accumulation of SNC1 proteins (Mang *et al.* 2012).

Discussion

Here we describe the use of bulked backcross segregants for next-generation sequencing to map and identify causal mutations in a simple and cost-effective way. As diagrammed in Figure 4, the general strategy is to first backcross a mutant isolated from a mutagenesis to the original starting strain (whether it be wild-type or already containing one or multiple mutations) to generate a segregating F_2 population. A small number of mutant and nonmutant plants are pooled separately and analyzed by next-generation sequencing. DNA

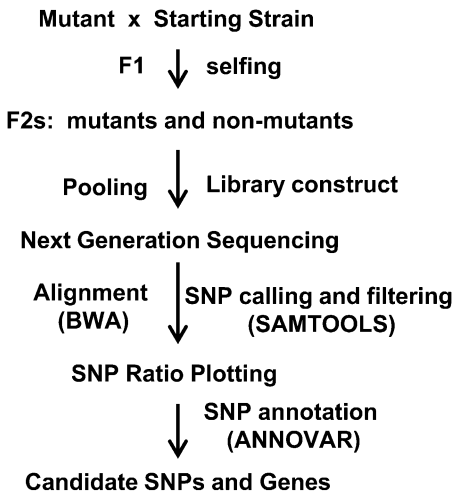

Figure 4 Diagram of mapping and cloning strategy with bulked segregants in backcross progenies. A mutant of interest will be backcrossed to its original starting strain and F_2 progenies will be scored for mutant phenotypes. Mutant plants and nonmutant plants will be separately pooled and their DNAs will be subject to next generation sequencing. The sequence reads will be aligned to reference genome, and SNP/INDEL will be called and filtered. SNP ratios will be plotted and mutation locations will be identified as peaks. Candidate SNPs will be annotated and the candidate genes will be tested and confirmed.

sequence polymorphisms induced by mutagens will be identified from sequence alignment to the reference genome, and ratios of nonreference *vs.* total SNP/INDELs in the mutant pool will be plotted along the chromosomes. The causal mutation and its associated nonreference SNP/INDELs should appear as a peak in this plot. Inspection of SNP/INDELs around the region in the mutant and nonmutant pools will identify recombination events that define the location of the causal mutation. The identity of causative genes will be confirmed by complementation test and/or characterizing additional mutant alleles.

This approach differs from the previously described methods using next-generation sequencing on bulked segregants in that it does not rely on polymorphisms existing between two different accessions for mapping. It complements those strategies by offering advantages in several scenarios. First, a mutant line does not need to be crossed to a different accession to generate a mapping population, which eliminates the potential confounding effects of accession differences. Second, for cloning of suppressor or enhancer mutations of an existing mutant, a mapping parent does not need to be created in a different accession. Rather, the starting strain (wild type or with the existing mutation) can be used for backcrosses. This method is also advantageous over direct sequencing of a mutant line or a backcrossed line. Although there was a case of gene cloning by directly comparing the whole genome sequencing of an EMS-induced mutant line to the reference genome (Zuryn *et al.* 2010), the success is dependent on a complete elimination of random mutations induced by EMS, which may or may not be achieved through multiple backcrosses. By sequencing pools of mutant and nonmutant segregants simultaneously in this approach, unassociated mutations will be identified as having a similar distribution in both pools, while the causal mutation and its linked mutations will be more prevalent in the mutant pool. In addition, even when the mutation is an epigenetic modification, the map position of the mutation can be defined on the basis of its linked SNP/INDELs.

We envision that this approach has a broad application especially in species where genome information for the second accession is not available (such as nontraditional model plants) and in cloning genes from double or even higher order of mutants. Nevertheless, this approach has several limitations. First, SNPs identified from this approach might be false positive due to misalignment of short reads onto the reference genome, while SNPs between accessions are usually validated by more than one approach or sample. Therefore it is necessary to inspect allele frequencies in two pools to identify false positive SNPs. Second, polymorphisms generated by mutagens such as EMS are likely much fewer than those between accessions. EMS induces about a 1-bp change in every 125 kb at the concentration used in mutagenesis, while there is one SNP every 3.3 kb between Col-0 and L*er* accessions of *Arabidopsis thaliana*. Therefore using polymorphisms between accessions has a higher statistic power in mapping than using EMS-induced polymorphisms. However, to fully take advantage of the high polymorphism density between accessions, a much larger number of segregants and a higher genome coverage are needed. For instance, to have recombination between the causal mutation and the nearest SNP that is 3.3 kb away, a total of 7000 plants would need to be fully sequenced assuming 200 kb per centimorgan in *Arabidopsis*. In this study, the mutant pool was sequenced to 11× coverage, potentially give a mapping resolution of 9 cM or 1.8–2.7 Mb, which was what we found in genome sequencing. The *int70* mutation was defined to a 2.3-Mb fragment and there was no recombination of the nine SNPs spanning the 1.6-Mb region. On the basis of the frequency of EMS mutations, the most cost-effective way would have been to sequence a pool of 50 mutant plants and a pool of 50 nonmutant plants each to a 50× genome coverage, as the resolution will be 2 cM or 400–600 kb, which would point to a smaller number of candidate SNPs.

We achieved a similar mapping resolution with a much smaller number of plants through next-generation sequencing as using 500 segregants in a traditional mapping population. Because we did not have a higher coverage of the genome or a larger number of mutant segregants, we were not able to resolve whether the apparent recombination suppression between crosses of two accessions would also occur in the backcross within the same accession. Further data mining using a different alignment method might reveal whether there is an inversion event in the *int70* mutant.

This study further supports our earlier findings that ABA deficiency enhances disease resistance and that it does so through affecting nuclear accumulation of NBS-LRR type of

proteins. The five *int* mutants we have isolated so far are *snc1-4*, *bon1-6*, *aba2-21*, *aba3-21*, and *aba3-22* (Zhu *et al.* 2010; Gou *et al.* 2011; Mang *et al.* 2012). The prevalence of ABA-deficient mutants in the *int* mutants indicates a critical regulation of ABA on TIR-NB-LRR R protein-mediated resistance especially at high temperatures. Decreasing and increasing the ABA amount have opposite effects on *SNC1*-mediated disease resistance (Figures 1 and 3), which most likely through its effect on the subcellular distribution of SNC1 with ABA levels inversely correlated with nuclear accumulation of SNC1 as observed in this study (Figure 3E) and an earlier study (Mang *et al.* 2012). Future study on the effect of ABA on the nuclear accumulation of R proteins will likely reveal novel intersecting mechanisms between biotic and abiotic stress responses.

Acknowledgments

We thank Xin Li for *snc1-1* seeds and the *Arabidopsis* Biological Resource Center for mutant seeds of *aba3-1*. This work is supported by National Science Foundation IOS-0919914 to J.H. and the National Science Foundation of China 31170254 to Y.Z.

Literature Cited

Abe, A., S. Kosugi, K. Yoshida, S. Natsume, H. Takagi *et al.*, 2012 Genome sequencing reveals agronomically important loci in rice using MutMap. Nat. Biotechnol. 30: 174–178.

Austin, R. S., D. Vidaurre, G. Stamatiou, R. Breit, N. J. Provart *et al.*, 2011 Next-generation mapping of Arabidopsis genes. Plant J. 67: 715–725.

Bittner, F., M. Oreb, and R. R. Mendel, 2001 ABA3 is a molybdenum cofactor sulfurase required for activation of aldehyde oxidase and xanthine dehydrogenase in Arabidopsis thaliana. J. Biol. Chem. 276: 40381–40384.

Cao, J., K. Schneeberger, S. Ossowski, T. Gunther, S. Bender *et al.*, 2011 Whole-genome sequencing of multiple Arabidopsis thaliana populations. Nat. Genet. 43: 956–963.

Colbert, T., B. J. Till, R. Tompa, S. Reynolds, M. N. Steine *et al.*, 2001 High-throughput screening for induced point mutations. Plant Physiol. 126: 480–484.

Cuperus, J. T., T. A. Montgomery, N. Fahlgren, R. T. Burke, T. Townsend *et al.*, 2010 Identification of MIR390a precursor processing-defective mutants in Arabidopsis by direct genome sequencing. Proc. Natl. Acad. Sci. USA 107: 466–471.

Dowell, R. D., O. Ryan, A. Jansen, D. Cheung, S. Agarwala *et al.*, 2010 Genotype to phenotype: a complex problem. Science 328: 469.

Elshire, R. J., J. C. Glaubitz, Q. Sun, J. A. Poland, K. Kawamoto *et al.*, 2011 A robust, simple genotyping-by-sequencing (GBS) approach for high diversity species. PLoS ONE 6: e19379.

Gan, X., O. Stegle, J. Behr, J. G. Steffen, P. Drewe *et al.*, 2011 Multiple reference genomes and transcriptomes for Arabidopsis thaliana. Nature 477: 419–423.

Gou, M., Z. Shi, Y. Zhu, Z. Bao, G. Wang *et al.*, 2011 The F-box protein CPR1/CPR30 negatively regulates R protein SNC1 accumulation. Plant J. 69: 411–420.

Jander, G., S. R. Norris, S. D. Rounsley, D. F. Bush, I. M. Levin *et al.*, 2002 Arabidopsis map-based cloning in the post-genome era. Plant Physiol. 129: 440–450.

Li, H., and R. Durbin, 2009 Fast and accurate short read alignment with Burrows-Wheeler transform. Bioinformatics 25: 1754–1760.

Li, H., B. Handsaker, A. Wysoker, T. Fennell, J. Ruan *et al.*, 2009 The Sequence Alignment/Map format and SAMtools. Bioinformatics 25: 2078–2079.

Lister, R., B. D. Gregory, and J. R. Ecker, 2009 Next is now: new technologies for sequencing of genomes, transcriptomes, and beyond. Curr. Opin. Plant Biol. 12: 107–118.

Lukowitz, W., C. S. Gillmor, and W. R. Scheible, 2000 Positional cloning in Arabidopsis. Why it feels good to have a genome initiative working for you. Plant Physiol. 123: 795–805.

Mang, H. G., W. Qian, Y. Zhu, J. Qian, H. G. Kang *et al.*, 2012 Abscisic acid deficiency antagonizes high-temperature inhibition of disease resistance through enhancing nuclear accumulation of Resistance proteins SNC1 and RPS4 in Arabidopsis. Plant Cell 24: 1271–1284.

Mardis, E. R., 2008 Next-generation DNA sequencing methods. Annu. Rev. Genomics Hum. Genet. 9: 387–402.

Pan, X., R. Welti, and X. Wang, 2008 Simultaneous quantification of major phytohormones and related compounds in crude plant extracts by liquid chromatography-electrospray tandem mass spectrometry. Phytochemistry 69: 1773–1781.

Peters, J. L., F. Cnudde, and T. Gerats, 2003 Forward genetics and map-based cloning approaches. Trends Plant Sci. 8: 484–491.

Schneeberger, K., S. Ossowski, C. Lanz, T. Juul, A. H. Petersen *et al.*, 2009 SHOREmap: simultaneous mapping and mutation identification by deep sequencing. Nat. Methods 6: 550–551.

Shendure, J., and H. Ji, 2008 Next-generation DNA sequencing. Nat. Biotechnol. 26: 1135–1145.

Uchida, N., T. Sakamoto, T. Kurata, and M. Tasaka, 2011 Identification of EMS-induced causal mutations in a non-reference Arabidopsis thaliana accession by whole genome sequencing. Plant Cell Physiol. 52: 716–722.

Wang, K., M. Li, and H. Hakonarson, 2010 ANNOVAR: functional annotation of genetic variants from high-throughput sequencing data. Nucleic Acids Res. 38: e164.

Wang, Y., Z. Bao, Y. Zhu, and J. Hua, 2009 Analysis of temperature modulation of plant defense against biotrophic microbes. Mol. Plant Microbe Interact. 22: 498–506.

Xiong, L., M. Ishitani, H. Lee, and J. K. Zhu, 2001 The Arabidopsis LOS5/ABA3 locus encodes a molybdenum cofactor sulfurase and modulates cold stress- and osmotic stress-responsive gene expression. Plant Cell 13: 2063–2083.

Yang, S., and J. Hua, 2004 A haplotype-specific Resistance gene regulated by *BONZAI1* mediates temperature-dependent growth control in Arabidopsis. Plant Cell 16: 1060–1071.

Zhang, Y., S. Goritschnig, X. Dong, and X. Li, 2003 A gain-of-function mutation in a plant disease resistance gene leads to constitutive activation of downstream signal transduction pathways in *suppressor of npr1–1, constitutive 1*. Plant Cell 15: 2636–2646.

Zhu, Y., W. Qian, and J. Hua, 2010 Temperature modulates plant defense responses through NB-LRR proteins. PLoS Pathog. 6: e1000844.

Zuryn, S., S. Le Gras, K. Jamet, and S. Jarriault, 2010 A strategy for direct mapping and identification of mutations by whole-genome sequencing. Genetics 186: 427–430.

Communicating editor: S. R. Poethig

GENETICS

Supporting Information
http://www.genetics.org/content/suppl/2012/06/19/genetics.112.141986.DC1

Gene Discovery Using Mutagen-Induced Polymorphisms and Deep Sequencing: Application to Plant Disease Resistance

Ying Zhu, Hyung-gon Mang, Qi Sun, Jun Qian, Ashley Hipps, and Jian Hua

DOI: 10.1534/genetics.112.141986

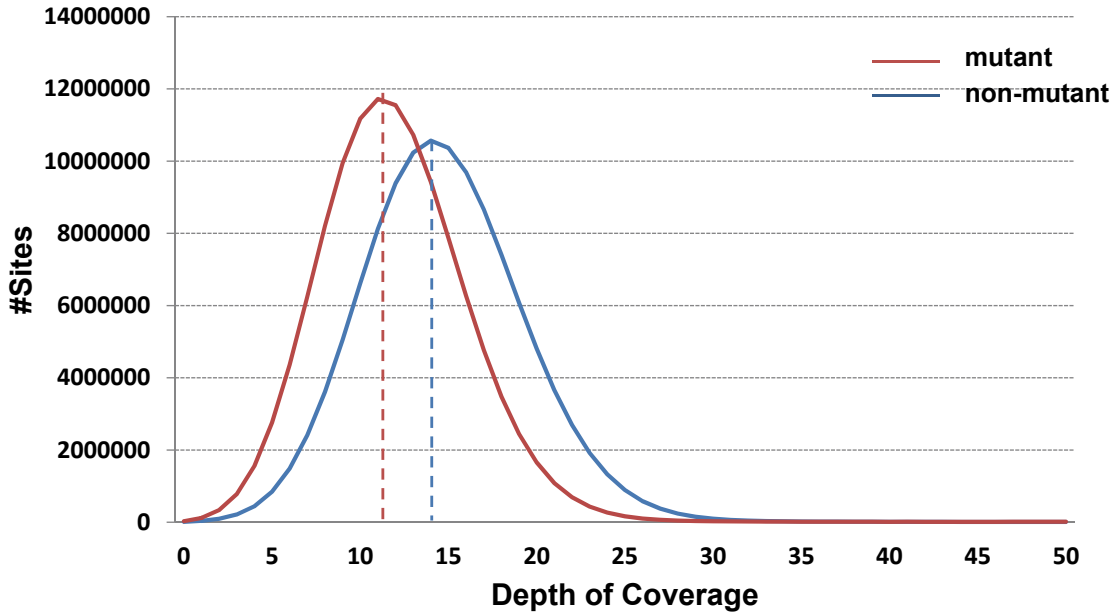

Figure S1 Distribution of the depth of coverage from single-end 51 bp sequencing on Illumina Hi-Seq. The mutant pool has on an average of 11 x coverage and the non mutant pool has on an average of 14 x coverage.

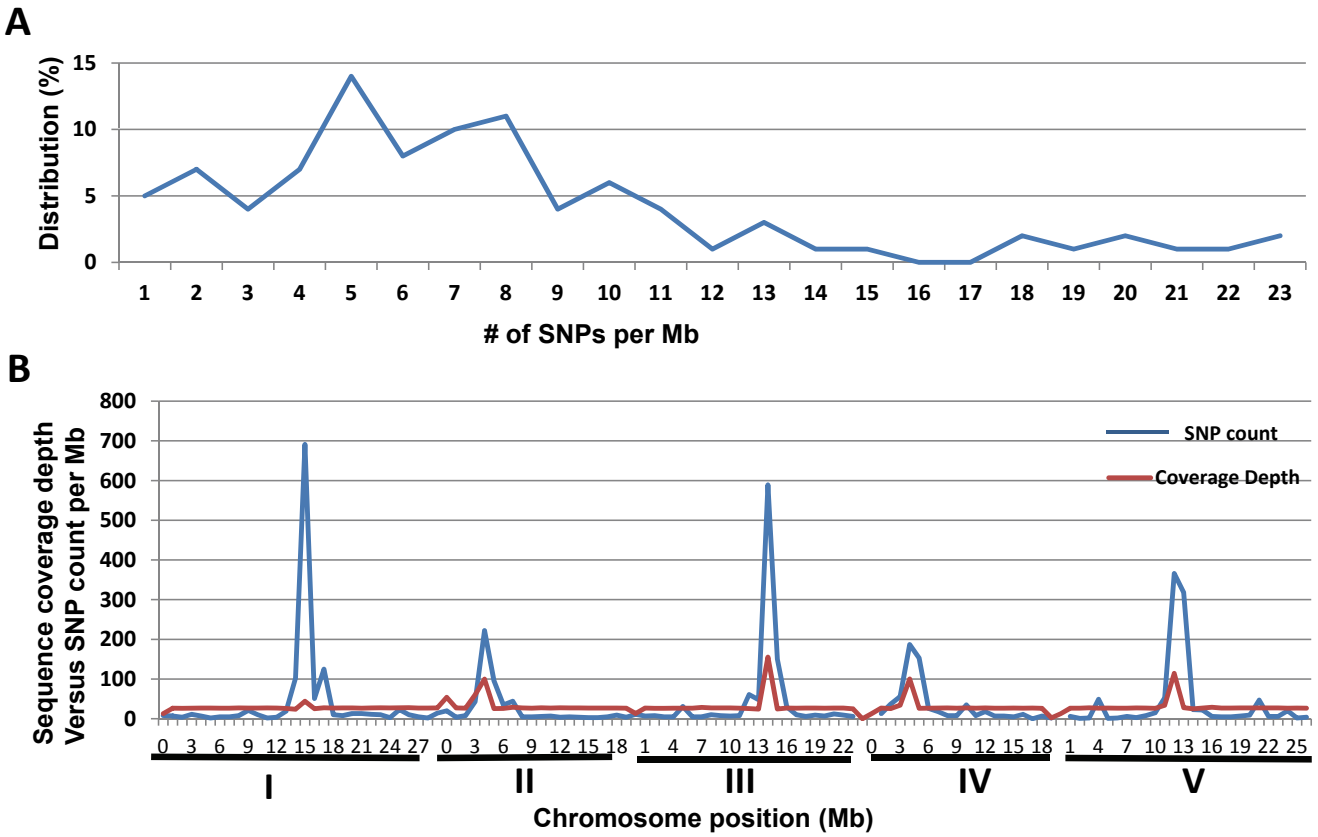

Figure S2 SNP distribution along the chromosomes. (A) Distribution of SNP count per Mb. Shown are the number of SNPs identified by SAMtool per Mb (X Axis) and the percentage of chromosome regions with that number of SNP count (Y Axis). The average SNP count is 8 per Mb across all regions. (B) The red line shows sequence coverage depth (sequence reads per site) and blue line shows the SNP count (number per 1 Mb sliding window). Several regions of chromosomes appear to have a high SNP count and most of them correlate with a high coverage depth, indicating a mis-calling of SNPs at the repetitive regions.

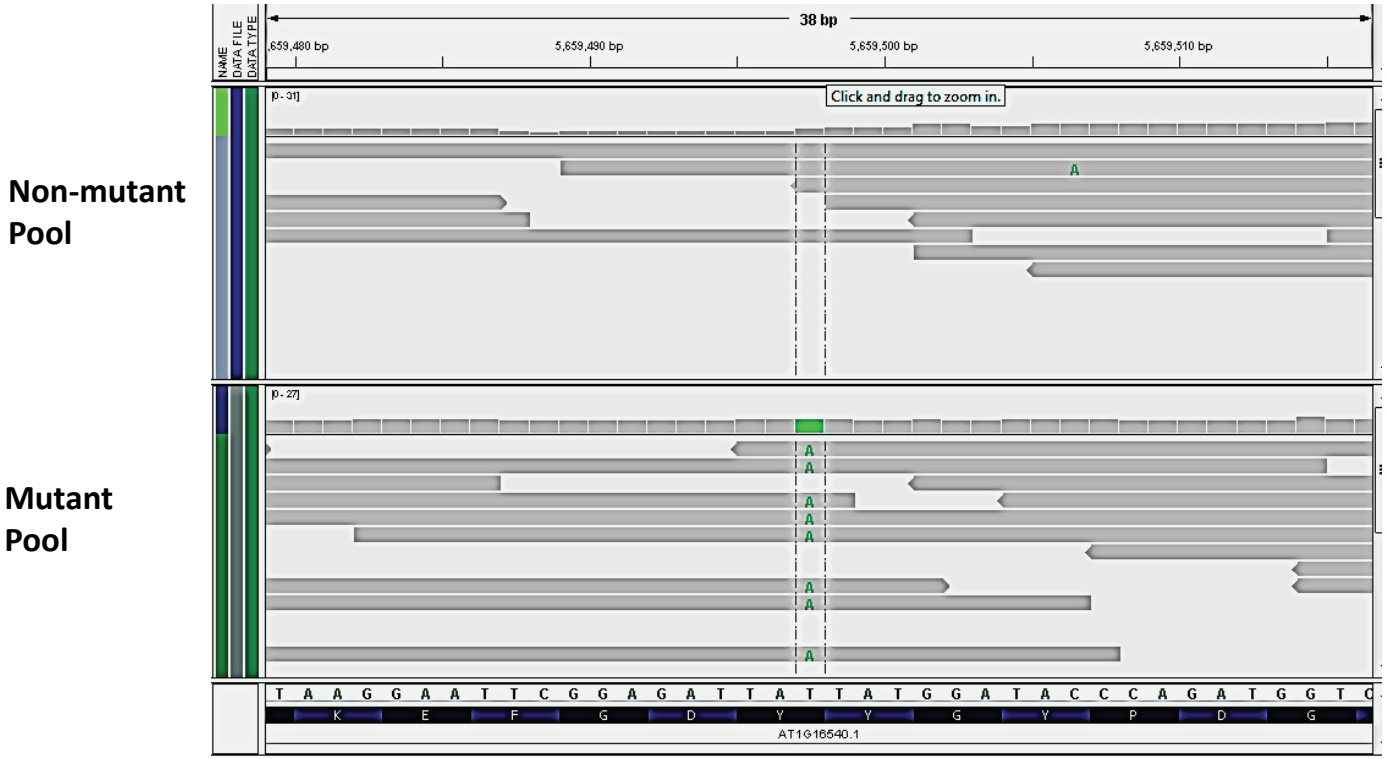

Figure S3 Sequence view at the region with the top candidate SNP. Sequence reads from the mutant pool and the non-mutant pool were viewed along the reference sequences with IGV software (http://www.broadinstitute.org/igv/). Non-reference alleles are indicated by green. All eight reads in the mutant pool has a non-reference base 'A' while all four reads in the non-mutant pool has the reference base of 'T'.